Micromaterials and Interfaces (2023) Volume 1 Issue 1
doi: 10.54517/mi.v1i1.2323

Asia Pacific Academy of Science Pte. Ltd.

ORIGINAL RESEARCH ARTICLE

Changes in the properties of composite materials based on hydroxyapatite

Ekaterina Anatolyevna Bogdanova*, Vladimir Mikhailovich Skachkov

Federal State Budgetary Institution of Science Institute of Solid State Chemistry UB RAS, 91 Pervomaiskaya Str., 620108 Ekaterinburg, Russia

*** Corresponding author:** Ekaterina Anatolyevna Bogdanova, chemi4@rambler.ru

ABSTRACT

The article discusses the possibility of obtaining a hardened composite material with a structure of different porosity based on nanostructured hydroxyapatite synthesized by precipitation from solution. In this work, mechanochemical synthesis of composite materials based on hydroxyapatite was carried out in a vibrating mill with simultaneous mixing and grinding of initial components and property-modifying additives (Si, Al, Zr, SiO_2, Al_2O_3, ZrO_2, 10–20 wt.% each) followed by annealing in the temperature range 200 °C–1000 °C. The synthesized samples were certified using modern physico-chemical methods of analysis. The influence of the qualitative and quantitative composition of the composite on the sintering processes, porosity, strength characteristics, degree of dispersion and morphology of the studied samples was shown. The peculiarities of chemical interaction of hydroxyapatite with reinforcing additives during heat treatment, the effect on grain size, and changes in the properties and structure during annealing were revealed. The effect of the phase composition and the amount of introduced additives on the strength characteristics of the investigated samples was shown. The optimum amount of reinforcing additives providing the production of a dense and strong composite material was determined.

Keywords: hydroxyapatite; porosity; composites; microhardness; silicon oxide; aluminum oxide; zirconium oxide

1. Introduction

Hydroxyapatite (HAP–$Ca_{10}(PO_4)_6(OH)_2$) is very similar to natural bone tissue in structure and chemical composition and has a pronounced osteotropic behavior in biological media[1–3], due to which it is widely used in medical practice for bone tissue replacement and restoration. HAP is used in various forms—microcapsules, powders, coatings, ceramic materials[4]. Of particular interest are HAP-ceramics, but a disadvantage of HAP-based bioceramics is their low mechanical strength limiting their application only to nonloaded areas[5], which does not suggest using them for elimination of bone tissue defects that experience regular significant mechanical loads. It is possible to increase the strength and fracture resistance of HAP-based biomaterials by mechanosynthesis of crystalline HAP with reinforcing additives[6–8]. When composite materials are produced, both during mechanosynthesis and heat treatment, the interaction between HAP and reinforcing phase takes place and the phase composition changes, which requires research into the physical and chemical processes occurring in the corresponding systems and the influence of the type and amount of the introduced component

ARTICLE INFO
Received: 28 September 2023 | Accepted: 24 October 2023 | Available online: 21 December 2023

CITATION
Bogdanova EA, Skachkov VM. Changes in the properties of composite materials based on hydroxyapatite. *Micromaterials and Interfaces* 2023; 1(1): 2323. doi: 10.54517/mi.v1i1.2323

on the medical and biological properties, microstructure, phase composition and mechanical characteristics of materials. In this work, the structure and properties of ceramic materials based on hydroxyapatite with the addition of powders of pure elements: Si, Al and Zr, and their oxides have been studied both individually and in double mixtures forming the system $Ca_{10}(PO_4)_6(OH)_2$–additive; the peculiarities of chemical interaction of HAP with reinforcing additives during heat treatment, their effect on the grain size, changes in the properties and structure during annealing have been revealed.

2. Experimental

The samples were prepared as follows: HAP of the composition $Ca_{10}(PO_4)_6(OH)_2$[9,10] was mixed together with powders of the corresponding additives introduced in the calculated amount without addition of homogenizer in a vibrating mill (MLW 4000 KM 1) with an agate mortar and a ball for 120 min. Composite materials $Ca_{10}(PO_4)_6(OH)_2$–additive were obtained as a result of mechanosynthesis. The initial HAP of the composition $Ca_{10}(PO_4)_6(OH)_2$[9] was used as a reference specimen. Thermal treatment was performed in a Nabertherm L 9/11 muffle furnace in the temperature range 200 ℃–1000 ℃ in steps of 200 ℃ at a heating rate of 10 ℃/min. X-ray diffraction analysis (XRD) was carried out on Shimadzu diffractometers (DRON-2.0) in CuKα radiation with angle interval $10 \leq 2\Theta \leq 70$, shooting step 0.03°, and 2 s time in point. Phases were identified using the Powder Diffraction File JCPDSD-ICDD PDF2 (sets 1-47)[10]. The microhardness of composite materials was measured according to Vickers on a PMT-3M microhardness meter with a load of 0.98 N (100 g) and loading time 10 s. The particle size was determined on a Horiba LA-950 universal laser express particle size distribution analyzer in the measuring range from 0.01 μm to 3000 μm with the maximal error 0.6%. The specific surface area was determined by the Brunauer-Emmett-Teller (BET) method of low-temperature nitrogen adsorption on a Gemini VII 2390 V1.03 (V1.03 t) automatic surface area and porosity analyzer, Micromeritics. The samples were preliminarily degassed on a VacPrep 061 Sample Degas System, Micromeritics, at T = 200 ℃ for 1 h. Morphological studies were performed using the scanning electron microscopy (SEM) method on a JEOL JSM 6390 LA microscope (Japan), magnification factor from ×5 to ×300000, resolution 3.0 nm at 30 kV.

3. Results and discussion

In the present work, in order to produce composite materials, a mechanochemical synthesis of $Ca_{10}(PO_4)_6(OH)_2$–additive (10–20 wt.% Si, Al, Zr, SiO_2, Al_2O_3, ZrO_2, and double additives SiO_2–ZrO_2, Al_2O_3–ZrO_2) was carried out in a mill while mixing and grinding the starting components. From the obtained mixtures, tablets were formed by uniaxial pressing on a hydraulic hand press at a pressure of 20 MPa without exposure. Then the samples were annealed in a wide temperature range (200 ℃–1000 ℃). Mechanochemical activation increases the highly dispersed state of the components, which is one of the ways to achieve strength and can lead to bond rupture, allowing new chemical compounds to form as a result of mechanochemical reactions[11].

The data on microhardness variation for the systems $Ca_{10}(PO_4)_6(OH)_2$–additive are presented in **Table 1**.

Table 1. Microhardness of components and HAP-based composites at different temperatures.

No.	Sample	Vickers hardness (HV), MPa					
		25 ℃	200 ℃	400 ℃	600 ℃	800 ℃	1000 ℃
1	HAP	52	71	53	75	87	183
2	$SiO_2 \cdot nH_2O$	30	59	42	49	103	247
3	Al_2O_3	35	63	33	56	68	197

Table 1. (*Continued*).

No.	Sample	Vickers hardness (HV), MPa					
		25 ℃	**200 ℃**	**400 ℃**	**600 ℃**	**800 ℃**	**1000 ℃**
4	ZrO_2	38	40	74	64	67	101
5	10%Si–HAP	99	135	86	216	97	115
6	20%Si–HAP	91	148	73	165	75	105
7	10%Al–HAP	95	56	56	85	158	-
8	20%Al–HAP	141	55	36	217	115	118
9	10%Zr–HAP	147	120	54	-	-	-
10	20%Zr–HAP	122	124	55	-	-	-
11	10%SiO_2·nH_2O–HAP	47	62	84	124	121	227
12	15%SiO_2·nH_2O–HAP	43	60	79	118	152	277
13	20%SiO_2·nH_2O–HAP	26	42	65	77	89	134
14	10%Al_2O_3–HAP	46	46	63	84	106	187
15	15%Al_2O_3–HAP	40	86	83	95	105	270
16	20%Al_2O_3–HAP	33	44	66	124	73	275
17	10%ZrO_2–HAP	33	73	63	143	104	270
18	15%ZrO_2–HAP	37	68	114	147	102	158
19	20%ZrO_2–HAP	38	71	91	134	113	97
20	15%SiO_2·nH_2O–5%ZrO_2–HAP	55	138	58	128	112	318
21	15%SiO_2·nH_2O–10%ZrO_2–HAP	51	111	41	107	173	292
22	15%Al_2O_3–5%ZrO_2–HAP	70	182	87	207	191	381
23	15%Al_2O_3–10%ZrO_2–HAP	69	123	135	195	148	206

From the table it is seen that the introduction of additives affects the behavior of the samples during annealing. Almost all samples showed a drop in microhardness after heat treatment at 400 ℃; at this temperature a restructuring of the HAP structure takes place and part of crystalline water is lost. It is known that HAP obtained by deposition from solutions partially decomposes with the formation of $Ca_3(PO_4)_2$–tricalcium phosphate (TCP) starting from the temperature 800 ℃[4,12], and the presence of reinforcing additives in composites prevents HAP decomposition into calcium phosphate and allows HAP to be stabilized below decomposition temperatures typical of HAP obtained by solid phase synthesis, as shown by comparison of XPA of heat treated initial HAP and composite materials. After annealing at 1000 ℃, initial HAP has increased hardness not only due to sintering, but also due to the formation of a small amount of TCP evenly distributed in the volume. This is not observed in other samples having a reinforcing additive in the composition. Not only the presence of additives in the composition of sample, but also their amount affect the variation in the phase composition during annealing. So, sample 7 containing 10 wt.% Al_2O_3 at 1000 ℃ promotes the formation of a large number of cracks. Samples 9 and 10 containing Zr crumble at 600 ℃ due to vigorous combustion of metallic Zr. As the annealing temperature rises, the degree of crystallinity of samples grows, as evidenced by the increased resolution and decreased width of XRD peaks, which is indirectly confirmed by the high microhardness after sintering at 1000 ℃. Annealing at temperatures above 800 ℃ leads to the densification of material due to removal of isolated pores and recrystallization, the grain size ranging from ~0.4–0.9 μm (800 ℃)

to ~1–4 μm (1000 °C). The SEM data (**Figure 1**) show the formation of large rounded crystals; the annealing produces a porous structure of composites $Ca_{10}(PO_4)_6(OH)_2$–additive.

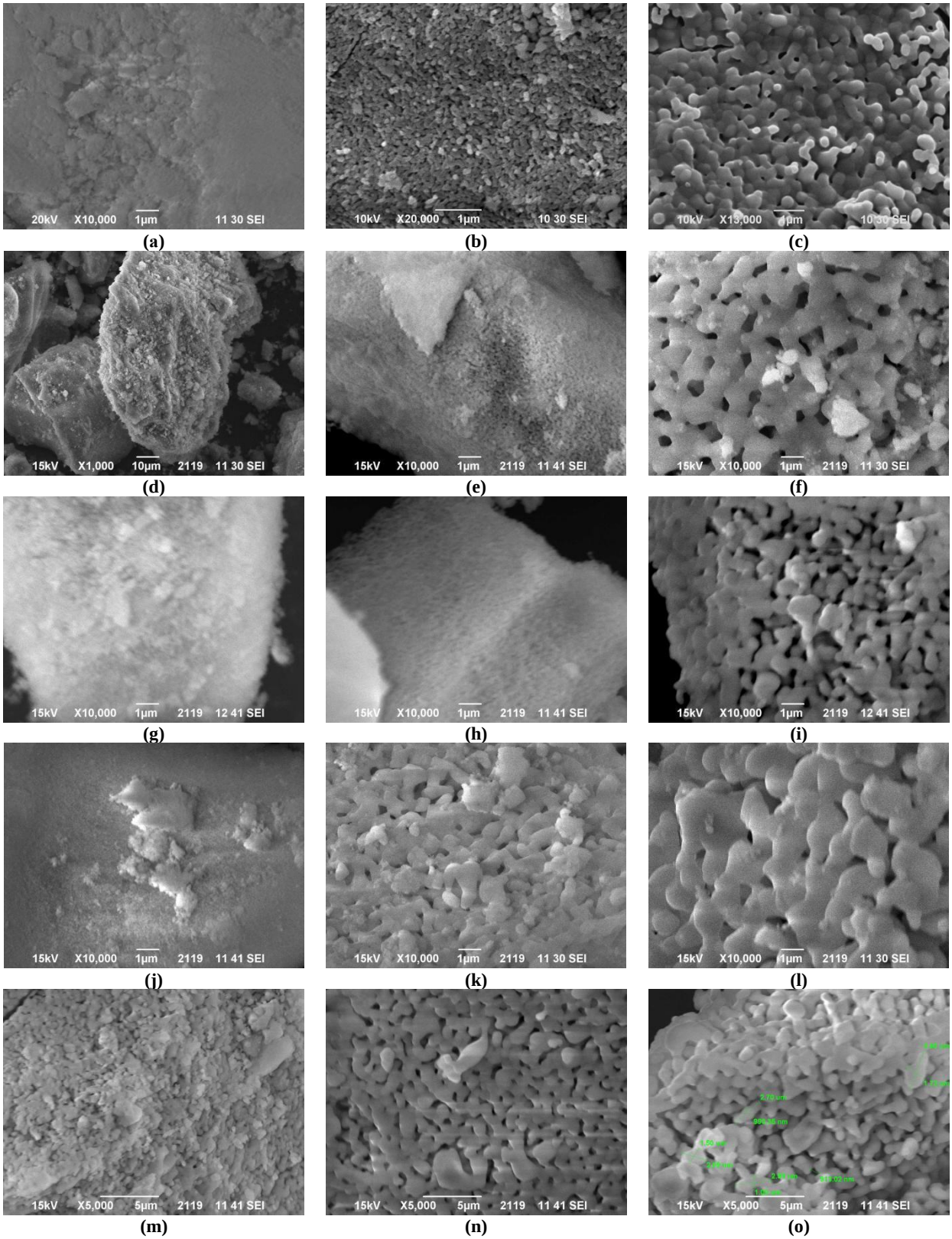

Figure 1. Morphology of initial substances and composites $Ca_{10}(PO_4)_6(OH)_2$–additive: **(a–c)** $Ca_{10}(PO_4)_6(OH)_2$; **(d–f)** 20%$SiO_2 \cdot nH_2O$–HAP; **(g–i)** 15%Al_2O_3–HAP; **(j–l)** 15%$SiO_2 \cdot nH_2O$–5%ZrO_2–HAP; **(m–o)** 15%Al_2O_3–5%ZrO_2–HAP annealed at different temperatures: a, d, g, j, m—600 °C; b, e, h, k, n—800 °C; c, f, I, l, o—1000 °C.

The morphological data obtained by SEM agree with the results of measurements of particle size distribution by laser diffraction, according to which the initial powders have a rather wide range of particle size distribution from 1 μm to 15 μm (the average particle diameter is ~1.8 μm).

Evaluation of the linear parameters of the samples made it possible to establish the dependence of the linear shrinkage of the sintered materials on their composition and annealing temperature (**Table 2**).

Table 2. Evaluation of linear shrinkage of samples at different temperatures.

Sample	**Linear shrinkage, Δ*h*, %**			
	400 ℃	**600 ℃**	**800 ℃**	**1000 ℃**
HAP	1.86	2.11	3.23	7.94
10%$SiO_2 \cdot nH_2O$–HAP	22.75	23.61	24.68	30.90
15%$SiO_2 \cdot nH_2O$–HAP	23.52	24.40	26.37	31.65
20%$SiO_2 \cdot nH_2O$–HAP	26.42	27.27	28.30	35.85
10%Al_2O_3–HAP	1.88	2.81	4.38	9.06
15%Al_2O_3–HAP	3.75	4.38	5.31	12.11
20%Al_2O_3–HAP	-	2.05	2.39	4.44
10%ZrO_2–HAP	3.83	4.17	6.41	11.21
20%Zr–HAP	16.0	16.0	16.92	19.38
15%$SiO_2 \cdot nH_2O$–5%ZrO_2–HAP	1.40	-	4.99	10.18
15%$SiO_2 \cdot nH_2O$–10%ZrO_2–HAP	1.24	1.95	4.42	9.37
15%Al_2O_3–5%ZrO_2–HAP	1.50	1.90	2.50	3.30
15%Al_2O_3–10%ZrO_2–HAP	1.00	1.50	1.80	2.80

The densification of composites $Ca_{10}(PO_4)_6(OH)_2$–additive begins at 400 ℃–600 ℃ and reaches a maximum at 800 ℃. The densification and changes in the specific surface and porosity of the material occurring during sintering were evaluated by the BET method (**Table 3**). When the annealing temperature increases, the surface becomes less developed; at 1000 ℃ the samples sinter, some samples have no pores, and samples containing silicic acid, on the contrary, have a porous surface formed during sintering, which will contribute to the intergrowth of tissue when creating implants. The presence of pores in composites and pure HAP can be explained by "burnout" of the surface, occurring during decomposition of crystalline water of the apatite phase.

Table 3. Results of specific surface area and porosity measurements of the samples.

Sample	**Specific surface area (S_{red}), m^2/g**		
	25 ℃	**800 ℃**	**1000 ℃**
HAP	98.8021	12.1417	0.4359
15%$SiO_2 \cdot nH_2O$–HAP	129.4320	27.5135	0.0195
15%Al_2O_3–HAP	107.2504	6.4800	4.7802
10%ZrO_2–HAP	94.9843	27.5135	0.0195
15%$SiO_2 \cdot nH_2O$–5%ZrO_2–HAP	153.9263	35.2488	4.8504
15%$SiO_2 \cdot nH_2O$–10%ZrO_2–HAP	118.9318	-	-

Table 3. (*Continued*).

Sample	**Specific surface area (S_{red}), m^2/g**		
	25 ℃	**800 ℃**	**1000 ℃**
15%Al_2O_3–5%ZrO_2–HAP	-	6.2101	3.8600
Pore area (S_p), m^2/g			
HAP	10.37	0.78	0.35
15%SiO_2·nH_2O–HAP	-	5.88	9.36
15%Al_2O_3–HAP	49.22	6.48	4.78
10%ZrO_2–HAP	-	-	-
15%SiO_2·nH_2O–5%ZrO_2–HAP	21.62	06.08	4.64
15%SiO_2·nH_2O–10%ZrO_2–HAP	3.95	-	-
15%Al_2O_3–5%ZrO_2–HAP	-	3.28	0.08
Pore volume (V_p), cm^3/g			
HAP	0.005483	0.000474	0.00020
15%SiO_2·nH_2O–HAP	-	0.003314	0.003864
15%Al_2O_3–HAP	0.001204	–	-
10%ZrO_2–HAP	-	-	-
15%SiO_2·nH_2O–5%ZrO_2–HAP	0.012568	0.003838	0.002681
15%SiO_2·nH_2O–10%ZrO_2–HAP	0.002101	-	-
15%Al_2O_3–5%ZrO_2–HAP	-	0.0001847	-

Densification of the material in the process of sintering and formation of new phases during the interaction of HAP and additives (except ZrO_2, which does not interact with HAP, but acts as disperse particles) promotes an increase in the strength of the composite material (**Table 1**).

4. Conclusion

In this work it was found that during mechanochemical activation and annealing an interaction occurs in the systems $Ca_{10}(PO_4)_6(OH)_2$–additive. A strong composite material with a uniform dense structure with a high degree of crystallinity, stable at 1000 ℃ was obtained in triple composites by introduction of 5 wt.% ZrO_2 and 15 wt.% SiO_2–nH_2O or Al_2O_3. The formation of interaction phases between HAP and SiO_2 or Al_2O_3 and the effect of dispersion hardening from ZrO_2 particles contribute to an increase in the strength of these samples. However, the amount of reinforcing additives has a strict ratio. An increase in ZrO_2 content in the composition of the material up to 10 wt.% and more promotes the formation of cracks and destruction of composites. The structural disordering that accompanies these phase transformations leads to a decrease in the microhardness of the material. The results obtained are consistent with the regularities described in the literature for ceramic materials.

Author contributions

Conceptualization, EAB and VMS; methodology, EAB; software, VMS; validation, EAB and VMS; formal analysis, EAB; investigation, EAB; resources, VMS; data curation, VMS; writing—original draft preparation, EAB; writing—review and editing, EAB; visualization, EAB; supervision, EAB; project administration, EAB; funding acquisition, EAB. All authors have read and agreed to the published version of

the manuscript.

Funding

This work was performed in accordance with the state assignment and research plants of ISSC UB RAS (No. AAAA-A19-119031890028-0).

Conflicts of interest

The authors declare no conflict of interest.

References

1. Bezrukov VM. Hydroxyapatite as a substrate for bone grafting: theoretical and applied aspects of the problem (Russian). Stomatologiya. 1996; 75(5): 7-12.
2. Akopyan GV. The use of osteoplastic materials in dental implantology (Russian). Assotsiatsiya stomatologov v Armenii. Theoretical and practical journal. 2012; 7(1): 10-14.
3. Stroganova EE. Novel technologies for production and application of bioceramics in restorative medicine (Russian). Steklo i keramika. 2008; 1: 36-38.
4. Barinov SM. Bioceramics based on phosphate cal'ciya (Russian). M.: Nauka; 2006. p. 204.
5. Kim HW. Effect of CaF2 on Densification and Properties of Hydroxyapatite–Zirconia Composites for Biomedical Applications. Biomaterials. 2002; 23: 4113–4121.
6. Krut'ko VK. Composites based on calcium phosphate foam ceramic and hydroxyapatite gel. Physical and Chemical Aspects of the Study of Clusters, Nanostructures and Nanomaterials. 2022; 14: 791-799. doi: 10.26456/pcascnn/2022.14.791
7. Bogdanova EA. Preparation of biocomposites based on nanoscale hydroxyapatite with titanium compounds. Physical and Chemical Aspects of the Study of Clusters, Nanostructures and Nanomaterials. 2022; 14: 521-530. doi: 10.26456/pcascnn/2022.14.521
8. Bogdanova EA. Development of composite mixtures based on hydroxyapatite and biogenic elements for the formation of bioactive coatings. Physical and Chemical Aspects of the Study of Clusters, Nanostructures and Nanomaterials. 2022; 14: 771-781. doi: 10.26456/pcascnn/2022.14.771
9. МПК C01B 25/32 Method for production of hydroxyapatite suspension. N. A. Sabirzyanov; applicant and rightholder–Institute of Solid State Chemistry of the Ural Branch of RAS (Russian). RF Patent 2406693, 20 December 2010.
10. Powder Diffraction File JCPDS-ICDD PDF-2 (Set 1-47). Available online: www.url: https://www.icdd.com/pdf-2/ (accessed on 15 May 2023).
11. Boldyrev VV. Mechanochemistry and mechanical activation of solids. Russ Chem Rev. 2006; 75(3): 177-189. doi: 10.1070/rc2006v075n03abeh001205
12. Bogdanova EA. Investigation into thermal stability of fluorine-substituted HAP (Russian). Materialovedeniye. 2015; 1: 52-56.